AIP Journal of Applied Physics

The stochastic dynamics of a nanobeam near an optomechanical resonator in a viscous fluid

S. Epstein and M. R. Paul

Citation: Journal of Applied Physics **114**, 144901 (2013); doi: 10.1063/1.4824297
View online: http://dx.doi.org/10.1063/1.4824297
View Table of Contents: http://scitation.aip.org/content/aip/journal/jap/114/14?ver=pdfcov
Published by the AIP Publishing

The stochastic dynamics of a nanobeam near an optomechanical resonator in a viscous fluid

S. Epstein[1] and M. R. Paul[2,a)]
[1]*Department of Engineering Science and Mechanics, Virginia Polytechnic Institute and State University, Blacksburg, Virginia 24061, USA*
[2]*Department of Mechanical Engineering, Virginia Polytechnic Institute and State University, Blacksburg, Virginia 24061, USA*

(Received 27 August 2013; accepted 19 September 2013; published online 8 October 2013)

We quantify the Brownian driven, stochastic dynamics of an elastic nanobeam immersed in a viscous fluid that is partially wrapped around a microdisk optical resonator. This configuration has been proposed as an optomechanical and nanoscale analog of the atomic force microscope [Srinivasan *et al.*, Nano Lett. **11**, 791 (2011)]. A small gap between the nanobeam and microdisk is necessary for the optomechanical transduction of the mechanical motion of the nanobeam. We compute the stochastic dynamics of the nanobeam in fluid for the precise conditions of the laboratory using deterministic finite element simulations and the fluctuation dissipation theorem. We investigate the dynamics of a nanobeam in water and in air and quantify the significance of the fluid-solid interaction between the nanobeam and the optical resonator. Our results in air show that, despite the complex geometry of the nanobeam, it can still be represented approximately as a damped simple harmonic oscillator. On the other hand, when the nanobeam is immersed in water there are significant deviations from the dynamics of a simple harmonic oscillator. The small gap between the nanobeam and the microdisk is found to be a significant source of additional dissipation. In air, the quality factor of the mechanical oscillation of the nanobeam is reduced by an order of magnitude due to the presence of the microdisk, however, the dynamics remain underdamped even in the presence of the microdisk. On the other hand, when placed in water, the dynamics without the microdisk is underdamped and with the microdisk the dynamics become strongly over damped. © *2013 AIP Publishing LLC*. [http://dx.doi.org/10.1063/1.4824297]

I. INTRODUCTION

Highly sensitive measurements of the mechanical motion of ultrasmall elastic objects in a viscous fluid are at the heart of many emerging technologies that have made significant impacts in a broad range of fields. A prominent example is the microscale cantilever that is central to atomic force microscopy (AFM).[1–3] Since the inception of the AFM there has been significant progress in using atomic force microscopy in fluid environments.[2–4] As technology progresses, there is increasing pressure to exploit the dynamics of mechanical oscillators that are much smaller than the typical micron scale AFM cantilever.[3,5–8] Among the advantages of using nanoscale elastic objects are improved time resolution due to much higher frequencies of oscillation (MHz and higher[9]) and also the possibility of much softer elastic objects with significantly improved force resolution.[10] However, there are significant experimental challenges in developing approaches to measure the motion of nanoscale elastic objects. For example, traditional AFM uses laser interferometry which is limited by the spot size of the laser.

A very promising approach is to measure the mechanical motion of the elastic object through its optomechanical coupling with a microdisk resonator.[11–13] This approach has yielded a number of exciting recent advances including measurements of mechanical motion at, or near, the standard quantum limit.[13,14] In this approach an elastic beam is placed is close proximity to an optical resonator. The elastic structure interacts with the evanescent wave of the microdisk[11] which can then be detected. This approach has been used to detect the motion of nanoscale beams with sub-femtometer/(Hz)$^{1/2}$ sensitivity in absolute displacement.[14]

In this paper, we explore in detail the Brownian driven mechanical motion of the nanobeam when the entire apparatus is immersed in a viscous fluid. As an important, and representative, example, we numerically investigate the stochastic dynamics for the geometry and configuration that has been explored experimentally by Srinivasan *et al.*[14] A schematic of the geometry of interest is shown in Fig. 1. A microdisk cavity optical resonator is located in the center with the nanobeam wrapped around the left portion of the microdisk. The nanoscale beam is attached to supports at four locations. The motion that we are interested in is the Brownian driven motion of the nanobeam that is in-plane with the nanobeam and microdisk. This particular geometry was chosen to stiffen out-of-plane modes which makes the in-plane mode the fundamental mode of oscillation for this structure. In essence, the structure is composed of two doubly clamped beams that are attached via the triangular section near the center of the nanobeam. This triangular section, for example, could serve as the tip for tapping mode type measurements. The small gap s_g between the nanobeam and the microdisk is necessary for the optomechanical coupling that is central for the measurement of the nanobeam dynamics. On the right hand side of the

a)Electronic mail: mrp@vt.edu.

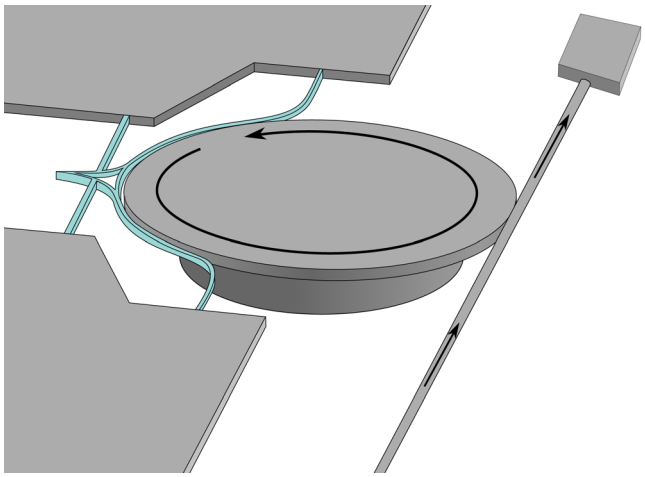

FIG. 1. A schematic of the nanobeam and microdisk optical resonator. The nanobeam is partially wrapped around the microdisk optical resonator. The nanobeam is attached to adjacent walls at four locations with the triangular tip of the nanobeam pointing to the left side of the microdisk optical resonator. The fundamental mode of mechanical vibration of the nanobeam is in-plane with the surface of the microdisk. On the right hand side of the microdisk is the fiber taper waveguide that leads to a photodetector. The arrows indicate the optical path. The geometry of the nanobeam is given in more detail in Fig. 2 and in Table I.

microdisk is a fiber taper waveguide where light travels from the bottom to the top where it is measured by a photodetector.

We now briefly describe the measurement approach and provide only the necessary details to place our work in context (for more details see Ref. 14). The fiber taper waveguide is sufficiently close to the microdisk that the evanescent tail of the optical mode is large enough in the waveguide to couple with the optical modes of the microdisk. The microdisk is a high-finesse oscillator with a typical quality factor of 10^5 or larger. The evanescent wave of the optical mode in the microdisk is large enough to couple with the mechanical vibrations of the nanobeam which can be detected at the photodetector.

In this paper, we quantify the mechanical motion of the nanobeam for the configuration of Fig. 1 when the entire apparatus is immersed in a viscous fluid. Specific properties describing the nanobeam are given in Table I. An in-plane projection of a portion of the geometry is shown in Fig. 2.

II. APPROACH

We compute the stochastic dynamics of the nanobeam using the thermodynamic approach of Paul and Cross.[15] We

TABLE I. Parameters describing the nanobeam. The geometry is shown in Fig. 2 where f_0 is the resonant frequency of the fundamental mode in vacuum, k is the spring constant, w is the width, h is the height, s_g is the gap thickness between the nanobeam and the microdisk, and $\langle x^2\rangle^{1/2}$ is the root-mean-squared magnitude of the Brownian fluctuations in displacement as measured at the tip of the nanobeam. The radius of the microdisk is $r_1 = 5.1\,\mu$m, $L_1 = 8.28\,\mu$m, $L_2 = 4.09\,\mu$m, $H_1 = 4.1\,\mu$m, and $H_2 = 0.6\,\mu$m. The nanobeam has a Young's modulus of $E = 174$ GPa and a density of $\rho_s = 2320\,\text{kg/m}^3$.

f_0 (MHz)	k (N/m)	w (nm)	h (nm)	s_g (nm)	$\langle x^2\rangle^{1/2}$ (pm)
7.81 MHz	2.15	260	100	8.28	44.9

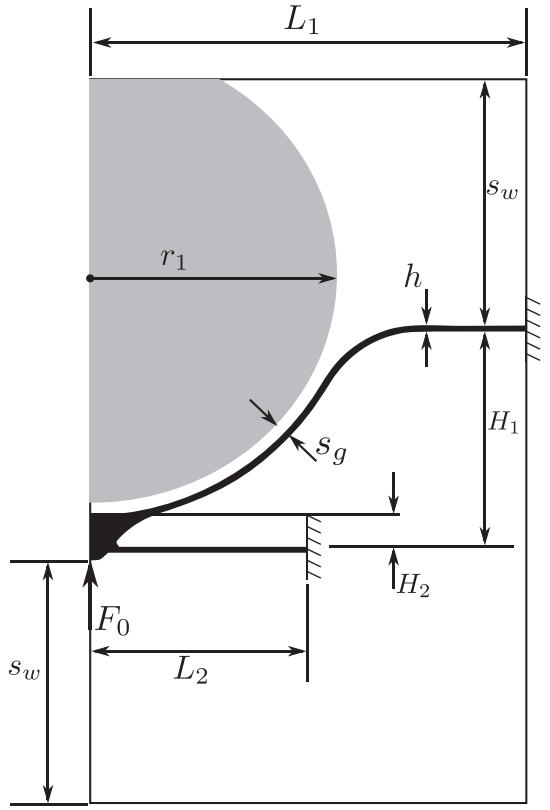

FIG. 2. The geometry of the nanobeam. The image shown represents the two-dimensional projection of the domain used in the numerical simulations. Several important length scales are as labelled. The microdisk is gray and the nanobeam is black. The location on the nanobeam where the step force removal of magnitude F_0 occurs is indicated at the tip of the nanobeam. The gap separation between the nanobeam and the microdisk is s_g and the distance to the nearest bounding wall in the numerical simulations is represented as s_w. The thickness of the nanobeam is h and the width of the nanobeam is w (the width is in the out-of-plane direction and is not shown). Specific values of the geometrical parameters are given in Table I.

provide only the essential details of the approach and refer the reader to Ref. 16 for more details. The approach has been used to quantify the stochastic dynamics of micro and nanoscale cantilevers in fluid,[15,16] the dynamics of a cantilever near a solid boundary,[17] and the dynamics of V-shaped cantilevers.[17] The approach has been validated by a direct comparison with experimental measurement for a variety of conditions.[16,18–21]

The essence of the approach is to compute the deterministic response of the system to the removal of a step-force and to then use the fluctuation-dissipation theorem to compute the autocorrelation and noise spectrum of equilibrium fluctuations in the nanobeam displacement. We use time-dependent, three-dimensional, and finite-element numerical simulations of the nanobeam-microdisk geometry shown in Fig. 2. We have used two planes of symmetry to greatly reduce the computational cost of the simulations. The motion of interest is in-plane with the nanobeam as shown in Fig. 2. The mode shape of the fundamental mode of oscillation is shown in Fig. 3. We point out that the thickness of the nanobeam is h as shown in Fig. 2. The important characteristic length with respect to the fluid motion, and its interaction with the nanobeam, is the width w which is in the direction perpendicular to the nanobeam motion.

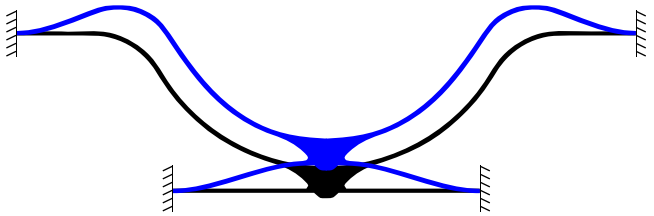

FIG. 3. A schematic of the fundamental mode of the nanobeam. The displacement is exaggerated for clarity.

Figure 1 is an accurate representation of the tip region of the nanobeam. In particular, we would like to draw attention to the hollow triangular geometry of the tip. In the numerical simulations we consider this region to be entirely made of the elastic material as shown in Fig. 2. At low Reynolds numbers, as is the case here, we expect the fluid solid interactions to be relatively insensitive to small geometrical features such as this and anticipate that this approximation incurs little error although we have not explored this aspect in detail.

In our numerical simulations, the microdisk is represented as a rigid object with a no-slip surface. As a result, we are neglecting the breathing mode dynamics of the microdisk. The breathing mode is at much higher frequency (>300 MHz) and at much smaller amplitudes.[14] We do not anticipate the breathing mode of the microdisk to have a significant effect upon the dynamics of the nanobeam. The bounding walls of the numerical domain are either symmetry planes or no-slip surfaces.

A force of magnitude F_0 is applied to the tip of the nanobeam at some time in the distant past as shown in Fig. 2. At time $t=0$, the force is removed and the nanobeam is allowed to return to equilibrium. The deterministic motion of the nanobeam tip as it returns to equilibrium $X(t)$ is directly related to the autocorrelation of equilibrium fluctuations of the nanobeam tip displacement $x(t)$. This relationship is found using the fluctuation-dissipation theorem and linear-response theory.[16] For the case of interest here it is,

$$\langle x(0)x(t)\rangle = k_B T \frac{X(t)}{F_0}, \tag{1}$$

where $\langle\rangle$ indicates an equilibrium ensemble average, k_B is Boltzmann's constant, and T is the temperature. The noise spectrum can be found immediately by taking a Fourier transform,

$$G(\omega) = 4\int_0^\infty \langle x(0)x(t)\rangle \cos(\omega t)dt. \tag{2}$$

Using the equipartition of energy it is straightforward to show that the root-mean-squared magnitude of the nanobeam displacement is very small, $\langle x^2\rangle^{1/2} = k_B T/k \approx 45\text{pm}$ where k is the equivalent spring constant given in Table I.

III. RESULTS AND DISCUSSION

We first explore the dynamics of the nanobeam when immersed in atmospheric air. The parameters describing the fluid, as well as several important nondimensional parameters, are given in Table II. In order to gain some insight into the physics of the fluid-solid interaction we initially quantify the dynamics of the nanobeam in the absence of the microdisk. It is insightful to describe the dominant physics for this particular parameter regime of high frequency and small amplitude motion of the nanobeam in fluid. An estimate for the Reynolds number of the fluid motion is

TABLE II. Important nondimensional parameters describing the dynamics of the nanobeam in a viscous fluid for the fluids of atmospheric air and water where R_0 is the frequency parameter, T_0 is the mass loading parameter, Wi is the Weissenberg number, R_u is the velocity based Reynolds number, and δ_0/s_g is the ratio of the Stokes length to the gap thickness. Also included are analytical predictions for the reduction in the resonant frequency in fluid ω_f^*/ω_0 and the quality factor for the fundamental mode Q^*. For air the density is $\rho_f = 1.28\,\text{kg/m}^3$ and the dynamic viscosity is $\mu_f = 1.9\times10^{-5}\text{kg/m-s}$. For water $\rho_f = 997\,\text{kg/m}^3$ and $\mu_f = 8.59\times10^{-4}\,\text{kg/m-s}$.

Fluid	R_0	T_0	Wi	R_u	s_g/δ_0	ω_f^*/ω_0	Q^*
Air	0.056	0.0011	0.01	6×10^{-4}	0.18	0.99	24
Water	0.96	0.88	$\ll1$	4×10^{-5}	0.77	0.23	0.68

$$R_u = \frac{\omega_0\langle x^2\rangle^{1/2} w}{\nu}, \tag{3}$$

where ν is the kinematic viscosity of the fluid. Using our parameters, and atmospheric air as the fluid, yields $R_u = 6\times10^{-4} \ll 1$. For this nanobeam $R_u \ll 1$ regardless of the fluid due to the extremely small amplitude of the oscillations. As a result, the convective nonlinearity of the fluid equations can be neglected despite the high frequency of oscillation.[16]

For an oscillating flow, a measure of the importance of molecular scale dynamics is given by the Weissenberg number $\text{Wi} = \omega\tau$ where ω is the frequency of oscillation of the nanobeam and τ is the fluid relaxation time scale.[22] For atmospheric air $\tau \approx \lambda/c \approx 0.2$ ns where λ is the mean free path of a fluid molecule between collisions and c is the speed of sound. For the resonator considered here, in atmospheric air, this yields $\text{Wi} \approx 0.01 \ll 1$ which indicates that the flow field can be treated as a continuum.[22] Although we have not explored this aspect further, we emphasize that it would be possible to use our general approach with a lattice-Boltzmann solver[23,24] for the fluid-solid interactions to quantify the dynamics in the $\text{Wi} \gtrsim 1$ limit if desired.

For the case of interest here we proceed by numerically simulating a free standing nanobeam immersed in air using the approach described in Sec. II. The autocorrelation of equilibrium fluctuations in nanobeam displacement is shown in Fig. 4(a) by the dashed line. In this figure, the autocorrelation is normalized by $k_B T/k$ and the time $\bar{t} = t/t_0$ has been normalized by the period of oscillation of the nanobeam at resonance in a vacuum.

The noise spectrum $\bar{G}(\tilde{\omega})$ is found using Eq. (2) and is shown in Fig. 4(b) by the dashed line. The noise spectrum has been normalized by its maximum value and is presented

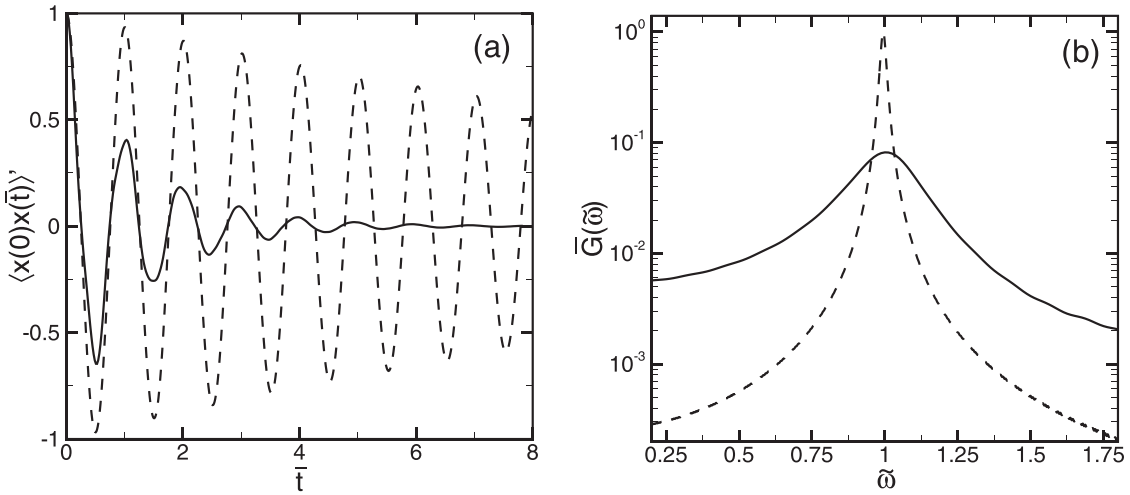

FIG. 4. The stochastic dynamics of the nanobeam when immersed in atmospheric air. The solid and dashed curves represent the nanobeam dynamics when the microdisk optical resonator is included and not included, respectively. (a) The autocorrelations of equilibrium fluctuations in tip displacement. The autocorrelation has been scaled by k_BT/k and is indicated by the prime notation. The scaled time $\bar{t} = t/t_0$ where $t_0 = 2\pi/\omega_0$ is the period of a single oscillation of the fundamental mode of the nanobeam in vacuum. (b) The noise spectrum of the displacement fluctuations. The noise spectrum $\bar{G}$ has been scaled by it maximum value in the absence of the microdisk.

as a function of the reduced frequency $\tilde{\omega} = \omega/\omega_0$. Fitting these results to the dynamics of a damped simple harmonic oscillator yields a quality factor of $Q = 44$ and a resonant frequency in fluid of $\tilde{\omega}_f = \omega_f/\omega_0 \approx 0.99$ where ω_f is the value of the frequency at the peak of the noise spectrum in Fig. 4(b).

The geometry of the nanobeam is quite complex and an analytical solution for this case is not available. However, it is insightful to compare these results with available analytical predictions for the stochastic dynamics of a long and thin beam of rectangular cross section where the noise spectrum is given by[15]

$$G(\tilde{\omega}) = \frac{4k_BT}{k}\frac{1}{\omega_0}\cdot\frac{T_0\tilde{\omega}\Gamma''(R_0\tilde{\omega})}{\left[(1-\tilde{\omega}^2(1+T_0\Gamma'(R_0\tilde{\omega})))^2+(\tilde{\omega}^2T_0\Gamma''(R_0\tilde{\omega}))^2\right]}. \tag{4}$$

In this approach, the fluid motion at each cross-section of the beam is represented as the fluid motion caused by an oscillating cylinder of diameter equal to the width w. The approximation of representing the rectangular cross-section as a circle is small (less than 10% error) for low Reynolds flows.[25] This approach does not include the effect of curvature of the nanobeam, the double beam configuration of the nanobeam structure, nor the details of the tip interactions with the fluid. The analytical description requires knowledge of two nondimensional parameters. The frequency parameter

$$R_0 = \frac{\omega_0 w^2}{4\nu}, \tag{5}$$

which plays the role of a frequency based Reynolds number and represents the ratio of local inertia forces to viscous forces. The mass loading parameter

$$T_0 = \frac{\pi}{4}\frac{\rho_f w}{\rho_s h}, \tag{6}$$

which represents the ratio of the mass a cylinder of fluid with a radius $w/2$ to the actual mass of the beam. The hydrodynamic function for an oscillating cylinder is found by solving the unsteady Stokes equation and is

$$\Gamma(\omega) = 1 + \frac{4iK_1(-i\sqrt{iR_0\tilde{\omega}})}{\sqrt{iR_0\tilde{\omega}}K_0(-i\sqrt{iR_0\tilde{\omega}})}, \tag{7}$$

where $i = \sqrt{-1}$, and K_0 and K_1 are Bessel functions. The real and imaginary parts of the hydrodynamic function are given by Γ' and Γ'', respectively. The values of the frequency and mass loading parameters for air are given in Table II.

Using the width w of the nanobeam as the characteristic length the analytical prediction of the quality factor is $Q^* = 24$ and the reduction of the resonant frequency is $\omega_f^*/\omega_0 = 0.99$. As expected, there is very little mass loading of the nanobeam when placed in air where $T_0 \ll 1$ and, as a result, there is very little shift of the resonant frequency to lower values such that $\tilde{\omega}_f \approx 1$.

It is interesting to note that $Q^* < Q$ indicating that the actual geometry used in the numerical simulations experiences less dissipation than the uniform straight beam approximation. Using the analytical predictions, we can determine the width of the equivalent beam that would yield the same dynamics. To accomplish this, we first determine the

required value of the frequency parameter R_0^* to yield the quality factor Q found by the numerical simulations. Next, by using Eq. (5), we can determine the required value of the beam width w^* for this case. Following this procedure yields $R_0^* \approx 2.2R_0$ which gives $w^*/w \approx 1.5$. Therefore, the complicated nanobeam geometry yields the same stochastic dynamics as a long, thin, and uniform beam with a width that is approximately 1.5 times larger than the width of the nanobeam. We anticipate that the double beam configuration of the nanobeam, with the bridging tip structure, has larger inertia and also results in fluid shielding effects that contribute to the larger quality factor.

We next consider the case of the nanobeam immersed in air with the microdisk present. The autocorrelations of the equilibrium fluctuations in the tip displacement of the nanobeam are shown in Fig. 4(a) by the solid line. The presence of the microdisk results in a significant increase in the fluid damping. There remains very little mass loading on the nanobeam $T_0 \ll 1$ and as a result $\tilde{\omega}_f \approx 1$. However, there is a dramatic reduction in the quality factor which is now $Q = 3.7$. The quality factor has reduced by an order of magnitude due to the presence of the microdisk. It is well known that the presence of nearby walls increases the fluid dissipation and will result in smaller values of the quality factor. This has been studied for cantilevers numerically[17] and analytically. The results from our numerical simulations using air as the fluid are given in Table III.[26,27]

An important length scale is the size of the unsteady viscous boundary layer caused by the oscillating object relative to the gap thickness. An estimate of the size of the unsteady viscous boundary layer is given by the Stokes length

$$\delta_0 = \sqrt{\frac{\nu}{\omega_0}}. \tag{8}$$

In Clark *et al.*,[17] it was shown that for a cantilever near a wall the reduction in the quality factor due to the presence of the wall begins when the separation is $s_g \lesssim 6\delta_0$. As shown in Table II, $s_g/\delta_0 = 0.18 \ll 6$ and the fluid interactions between the nanobeam and the microdisk are expected to be significant. The significant increase in fluid damping can also be seen in the noise spectrum shown by the solid line in Fig. 4(b). For ease of comparison, the maximum value of the noise spectrum has been normalized by the same value used to normalize the noise spectrum in the absence of the microdisk. Using the analytical theory available for a straight uniform beam, we can again find the required width of the nanobeam to achieve the same quality factor. In this case, $R_0^*/R_0 = 0.095$ which yields $w^*/w = 0.31$.

TABLE III. Results from numerical simulation of the nanobeam in air where ω_f is the resonant frequency in fluid, ω_0 is the resonant frequency in vacuum, and Q is the quality factor of the fundamental mode. These quantities are found by fitting the numerical results to an underdamped simple harmonic oscillator.

Fluid	ω_f/ω_0	Q	
Air	0.99	44	Without microdisk
Air	0.99	3.7	With microdisk

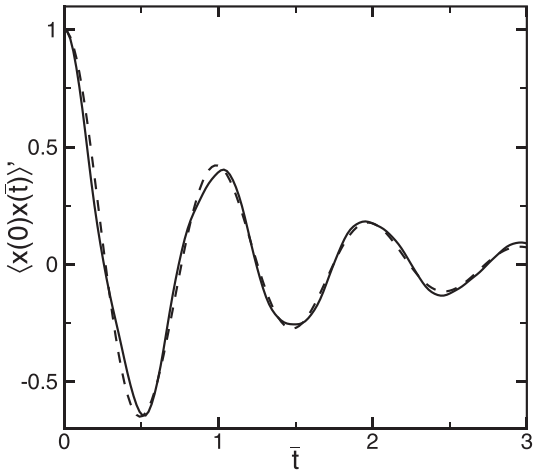

FIG. 5. The stochastic dynamics of the nanobeam when immersed in atmospheric air in the presence of the microdisk. The solid curve is the result from numerical simulation and the dashed line is a curve-fit using a simple harmonic oscillator approximation. The notation used is the same as that of Fig. 4(a).

In the presence of the microdisk in air, approximating the nanobeam as an underdamped simple harmonic oscillator remains valid. In Fig. 5, we show the autocorrelations from numerical simulation by the solid line and also the simple harmonic oscillator curve fit as the dashed line. Although some deviations are evident between the fitted curve and the numerical results it is clear that these deviations are quite small.

We next explore the dynamics when the nanobeam is immersed in water. This case is particularly interesting since there is significant pressure to develop nanoscale oscillators for use in making measurements on biological samples in aqueous environments. Figure 6 illustrates the dynamics in water where the dashed lines are the results without the microdisk and the solid lines are for results with the microdisk.

Without the microdisk, the dynamics are underdamped and using the simple harmonic oscillator analogy yields a quality factor of $Q = 1.6$ and a reduction of the resonant frequency of $\tilde{\omega}_f = 0.58$ as shown in Table IV. In this case, it is difficult to fit the dynamics with a simple damped harmonic oscillator. Both the added mass and the fluid damping are frequency dependent and when placed in water these effects become significant making this analogy only approximate.

The analytical predictions using a straight uniform beam are $Q^* = 0.68$ and $\omega_f/\omega_0 = 0.23$ as shown in Table II. Again the actual geometry has a larger quality factor than the predicted value where $Q > Q^*$. In this case, there are two contributing factors. First is the geometry where the curvature of the nanobeam and its double beam configuration yields less fluid damping than for a single straight beam oscillating in a fluid. Second is the amount of mass loading on the nanobeam due to the added mass of the fluid. The reduction of the resonant frequency for the theoretical prediction is much lower than what is found for the actual geometry where $\omega_f^*/\omega_0 < \omega_f/\omega_0$. This indicates that the added mass due to the fluid motion is less for the actual geometry than for the straight uniform nanobeam. We could not find an equivalent straight nanobeam to yield the same values of the quality factor and the reduction in resonant frequency.

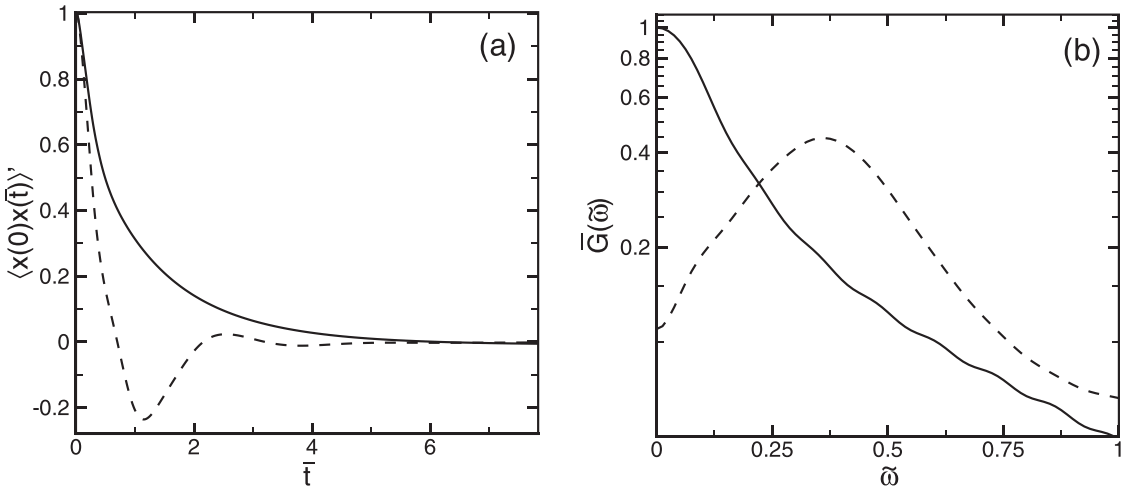

FIG. 6. The stochastic dynamics of the nanobeam when immersed in water. (a) The autocorrelation of equilibrium fluctuations in nanobeam displacement. (b) The noise spectra. This figure uses the same notation and scaling as discussed in Fig. 4.

TABLE IV. Results from numerical simulation of the nanobeam in water. The dynamics in the absence of the microdisk are underdamped. When the microdisk is included the dynamics are overdamped and the damped simple harmonic oscillator description is no longer accurate.

Fluid	ω_f/ω_0	Q	
Water	0.58	1.6	Without microdisk
Water	NA	$<1/2$	With microdisk

When the microdisk is included the dynamics become strongly overdamped with $Q \ll 0.5$ as indicated in Fig. 6. In this case, the gap separation is still small where $s_g/\delta_0 = 0.77 < 6$ which again indicates the importance of the interactions with the microdisk. The dynamics now significantly deviate from that of a damped simple harmonic oscillator. As a result of the strong over damping, it would be difficult to use the current design in water if the experimental approach requires a well defined peak. However, this could be improved by increasing the value of R_0 which would increase the quality factor (c.f. Ref. 28). For example, R_0 could be increased by stiffening the fundamental mode to increase the value of the resonant frequency. This could be done by shortening L_2 or increasing the height h.

IV. CONCLUSION

We have computed the stochastic dynamics of a nanobeam with a complex geometry that is placed near a micron scale optical disk. Despite the complexity of the problem, we are able to compute the stochastic dynamics using only deterministic calculations and the fluctuation-dissipation theorem. Our results indicate that the presence of the microdisk is a significant source of dissipation. In air, this reduces the quality factor of the oscillations by an order of magnitude. In water, this results in a strongly over damped oscillator. An analytical theory using a straight and uniform beam approximation can be used to gain some insight into the dynamics. The complex geometry and the small gap between the nanobeam and the microdisk result in deviations from simple harmonic oscillator behavior. Our numerical results do not rely on this approximation and qualitatively represent what would be measured in experiment. We would like to point out that externally driven dynamics, as would be the case for tapping mode type operation, would be qualitatively similar to the results we present here (c.f. Refs. 16 and 29). Our results quantify the dynamics of this emerging nanoscale technology and we anticipate that our findings will be useful in guiding future theoretical and experimental efforts to push these ideas further.

ACKNOWLEDGMENTS

S.E. would like to acknowledge many useful interactions with Vladimir Aksyuk during the initial stages of this work.

[1]G. Binnig, C. F. Quate, and C. Gerber, Phys. Rev. Lett. **56**, 930 (1986).
[2]R. García and R. Pérez, Surf. Sci. Rep. **47**, 197 (2002).
[3]A. Raman, J. Melcher, and R. Tung, Nanotoday **3**, 20 (2008).
[4]B. L. Smith, Prog. Biophys. Mol. Biol. **74**, 93 (2000).
[5]D. A. Walters, J. P. Cleveland, N. H. Thomson, P. K. Hansma, M. A. Wendman, G. Gurley, and V. Elings, Rev. Sci. Instrum. **67**, 3583 (1996).
[6]M. B. Viani, T. E. Schäffer, and A. Chand, J. Appl. Phys. **86**, 2258 (1999).
[7]H. Craighead, Science **290**, 1532 (2000).
[8]K. L. Ekinci and M. L. Roukes, Rev. Sci. Instrum. **76**, 061101 (2005).
[9]X. L. Feng, C. J. White, A. H. Hajimir, and M. L. Roukes, Nature Nanotech **3**, 342 (2008).
[10]J. L. Arlett, M. R. Paul, J. Solomon, M. C. Cross, S. E. Fraser, and M. L. Roukes, Lect. Notes Phys. **711**, 241 (2007).
[11]T. J. Kippenberg and K. J. Vahala, Opt. Express **15**, 17172 (2007).
[12]M. Li, W. Pernice, C. Xiong, T. Baehr-Jones, M. Hochberg, and H. Tang, Nature **456**, 480 (2008).
[13]G. Anetsberger, O. Arcizet, Q. P. Unterreithmeier, R. Riviere, A. Schliesser, E. M. Weig, J. P. Kotthaus, and T. J. Kippenberg, Nature Phys. **5**, 909 (2009).
[14]K. Srinivasan, H. Miao, M. T. Rakher, M. Davanco, and V. Aksyuk, Nano Lett. **11**, 791 (2011).
[15]M. R. Paul and M. C. Cross, Phys. Rev. Lett. **92**, 235501 (2004).
[16]M. R. Paul, M. T. Clark, and M. C. Cross, Nanotechnology **17**, 4502 (2006).
[17]M. T. Clark and M. R. Paul, J. Appl. Phys. **103**, 094910 (2008).
[18]R. J. Clarke, O. E. Jensen, J. Billingham, A. P. Pearson, and P. M. Williams, Phys. Rev. Lett. **96**, 050801 (2006).
[19]C. D. F. Honig, M. Radiom, B. A. Robbins, J. Y. Walz, M. R. Paul, and W. A. Ducker, Appl. Phys. Lett. **100**, 053121 (2012).
[20]M. Radiom, B. A. Robbins, C. D. F. Honig, J. Y. Walz, M. R. Paul, and W. A. Ducker, Rev. Sci. Instrum. **83**, 043908 (2012).

[21]D. Seo, M. R. Paul, and W. A. Ducker, Rev. Sci. Instrum. **83**, 055005 (2012).
[22]K. L. Ekinci, D. M. Karabacak, and V. Yakhot, Phys. Rev. Lett. **101**, 264501 (2008).
[23]Y. Shi and J. E. Sader, Phys. Rev. E **81**, 036706 (2010).
[24]C. E. Colosqui, D. M. Karabacak, K. L. Ekinci, and V. Yakhot, J. Fluid Mech. **652**, 241 (2010).
[25]J. E. Sader, J. Appl. Phys. **84**, 64 (1998).
[26]C. P. Green and J. E. Sader, Phys. Fluids **17**, 073102 (2005).
[27]R. J. Clarke, S. M. Cox, P. M. Williams, and O. E. Jensen, J. Fluid Mech. **545**, 397 (2005).
[28]M. M. Villa and M. R. Paul, Phys. Rev. E **79**, 056314 (2009).
[29]M. T. Clark, J. E. Sader, J. P. Cleveland, and M. R. Paul, Phys. Rev. E **81**, 046306 (2010).